Title

Dependence of Morphology, Shear Modulus, and Conductivity on the Composition of Lithiated and Magnesiated Single-Ion-Conducting Block Copolymer Electrolytes

Journal

Macromolecules, 50(21)

ISSN

0024-9297

Authors

Rojas, Adriana A
Thakker, Kanav
McEntush, Kyle D
et al.

Publication Date

2017-11-14

DOI

10.1021/acs.macromol.7b01686

Peer reviewed

Macromolecules

Article

Cite This: Macromolecules 2017, 50, 8765-8776

pubs.acs.org/Macromolecules

Dependence of Morphology, Shear Modulus, and Conductivity on the Composition of Lithiated and Magnesiated Single-Ion-Conducting Block Copolymer Electrolytes

Adriana A. Rojas,[†,‡,§] Kanav Thakker,[†] Kyle D. McEntush,[†] Sebnem Inceoglu,[‡,§] Gregory M. Stone,[∥] and Nitash P. Balsara*[,†,‡,§]

[†]Chemical and Biomolecular Engineering Department, University of California, Berkeley, Berkeley, California 94720, United States

[‡]Materials Science Division and [§]Joint Center for Energy Storage, Lawrence Berkeley National Laboratory, Berkeley, California 94720, United States

[∥]Malvern Instruments Inc., 117 Flanders Road, Westborough, Massachusetts 01581, United States

Supporting Information

ABSTRACT: Single-ion-conducting block copolymers are of considerable interest as electrolytes for battery systems, as they eliminate overpotentials due to concentration gradients. In this study, we characterize a library of poly(ethylene oxide) (PEO)-based diblock copolymers where the second block is poly(styrene-4-sulfonyltrifluoromethylsulfonyl)imide with either cation: univalent lithium or divalent magnesium counterions (PEO−PSLiTFSI or PEO−P[(STFSI)$_2$Mg]). The PEO chain length is held fixed in this study. Polymers were synthesized in matched pairs that were identical in all aspects except for the identity of the counterion. Using rheology, SAXS, DSC, and AC impedance spectroscopy, we show that the dependence of morphology, modulus, and conductivity on composition in these charged copolymer systems is fundamentally different from uncharged block copolymers. At a given frequency and temperature, the shear moduli of the magnesiated copolymer systems were approximately 3−4 orders of magnitude higher than those of the matched lithiated pair. The shear moduli of all of the lithiated copolymers showed liquid-like rheological features while the magnesiated copolymers did not. All of the lithiated copolymers were completely disordered (homogeneous), consistent with the observed rheological properties. As expected, the moduli of the lithiated copolymers increased with increasing volume fraction of the ion-containing block (ϕ_{PSTFSI}), and the conductivity decreased with ϕ_{PSTFSI}. However, the magnesiated copolymers followed a distinct trend. We show that this was due to the presence of microphase separation in the regime $0.21 \leq \phi_{PSTFSI} \leq 0.36$, and the tendency for microphase separation became weaker with increasing ϕ_{PSTFSI}. The magnesiated copolymer with $\phi_{PSTFSI} = 0.38$ was homogeneous. The morphological, rheological, and conductivity properties of these systems are governed by the affinity of the cations for PEO chains; homogeneous systems are obtained when the cations migrate from the ion-containing block to PEO.

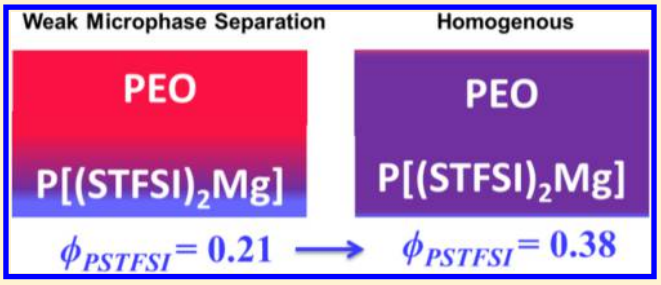

INTRODUCTION

The phase behavior of uncharged A−B diblock copolymer melts is well-established.[1−5] We consider a hypothetical experiment wherein the length (or molecular weight) of the A block is held fixed while the molecular weight of the B block is systematically increased such that the volume fraction of B, ϕ_B, increases from about 0.2 to 0.4 (B is the minor component). We expect to see an increasing tendency to form ordered phases with increasing ϕ_B. The total chain length increases with increasing ϕ_B in our hypothetical experiment, and this is known to promote ordering.[1] The block copolymer becomes more symmetric with increasing ϕ_B, and this is also known to promote ordering.[1] One could use this information to predict changes in rheological properties in our hypothetical experiment. If the B block is more rigid than the A block, one would predict that the shear moduli at a given frequency and temperature would increase with ϕ_B. It is worth noting that increasing chain length and promoting order also results in an increase in the shear moduli; in fact, an increase in the moduli is often used to detect a disorder-to-order transition.[6−10]

This paper deals with single-ion-conducting block copolymers comprising a nonionic block (A) and an ion-containing block (B). These systems are of interest for their potential application in rechargeable batteries, as they eliminate overpotentials due to concentration gradients.[11−18] Ion-containing block copolymers have been the subject of numerous recent theoretical studies.[19−24] It has been shown that Coulombic effects can fundamentally alter the thermodynamics of block copolymers. In our work, the ion-containing block comprises poly(styrene-4-sulfonyltrifluoromethylsulfonyl)imide repeat

Received: August 3, 2017
Revised: October 2, 2017
Published: October 18, 2017

DOI: 10.1021/acs.macromol.7b01686
Macromolecules 2017, 50, 8765−8776

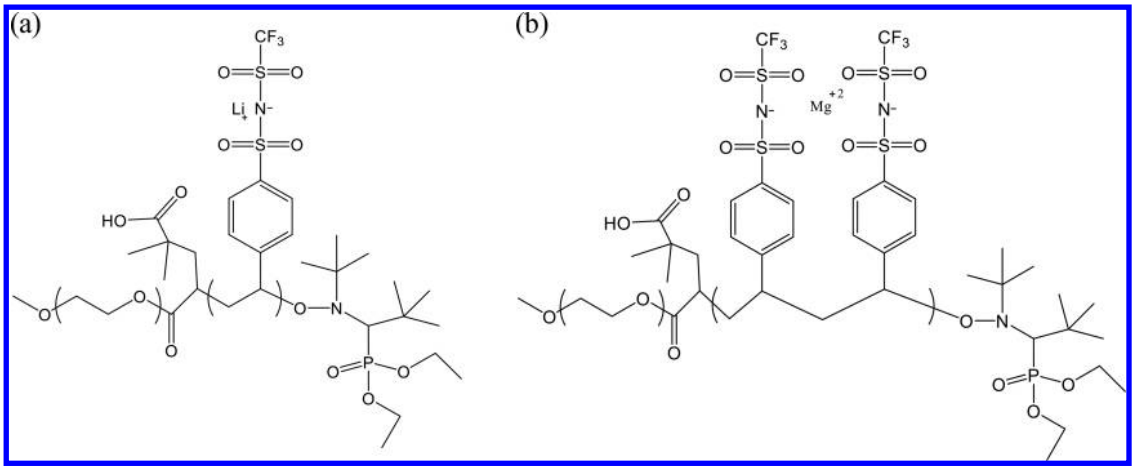

Figure 1. Chemical structures of (a) PEO−PSLiTFSI copolymer and (b) PEO−P[$(STFSI)_2Mg$].

Table 1. Characteristics of Polymers[a]

polymer name	M_n PEO	M_n PSLiTFSI or P[$(STFSI)_2Mg$]	$Đ$	r	ϕ_{PEO}	ϕ_{PSTFSI}
PEO 9.5	9.5	0	1.09	0	1	0
PEO−PSLiTFSI(9.5−3.5)	9.5	3.5	1.15	0.05	0.79	0.21
PEO−PSLiTFSI(9.5−4.9)	9.5	4.9	1.15	0.07	0.73	0.27
PEO−PSLiTFSI(9.5−7.6)	9.5	7.6	1.14	0.11	0.64	0.36
PEO−PSLiTFSI(9.5−8.3)	9.5	8.3	1.15	0.12	0.62	0.38
PEO−P[$(STFSI)_2Mg$](9.5−3.6)	9.5	3.6	1.15	0.025	0.79	0.21
PEO−P[$(STFSI)_2Mg$](9.5−5.0)	9.5	5.0	1.15	0.035	0.73	0.27
PEO−P[$(STFSI)_2Mg$](9.5−7.7)	9.5	7.7	1.14	0.055	0.64	0.36
PEO−P[$(STFSI)_2Mg$](9.5−8.5)	9.5	8.5	1.15	0.06	0.62	0.38

[a] M_n PEO = number-average molecular weight of the PEO block; M_n PSLiTFSI = number-average molecular weight of the PSLiTFSI block, M_n P[$(STFSI)_2Mg$] = number-average molecular weight of the P[$(STFSI)_2Mg$] block; $Đ$ = dispersity; r = $[Li^+][EO]^{-1}$ for the PEO−PSLiTFSI copolymers, and r = $[Mg^{2+}][EO]^{-1}$ for the magnesiated copolymers; ϕ_{PEO} = volume fraction of PEO block; ϕ_{PSTFSI} = volume fraction of the ion-containing block.

units with either lithium (univalent) or magnesium (divalent) counterions, PSLiTFSI or P[$(STFSI)_2Mg$]. The nonionic block is poly(ethylene oxide) (PEO). The chemical structures of the block copolymers are shown in Figure 1. Our work on this class of materials is motivated by the pioneering work of Bouchet et al., who first proposed the possibility of using these systems for battery applications.[11]

Here we fix the molecular weight of the PEO block (9.5 kg mol^{-1}) and study the properties of the block copolymers as a function of increasing molecular weight of the ion-containing block. The volume fraction of the ion-containing block, ϕ_{PSTFSI}, is thus increased from 0.21 to 0.38. We focus our attention to temperatures above the melting temperature of the PEO block. We show that the lithiated systems are disordered at all temperatures and all compositions, consistent with our previous studies on low molecular weight samples.[16,17] In contrast, the magnesiated samples show signatures of microphase separation in the regime $0.21 < \phi_{PSTFSI} < 0.36$, and the tendency for microphase separation becomes weaker with increasing ϕ_{PSTFSI}. These signatures disappear when ϕ_{PSTFSI} is increased from 0.36 to 0.38. The consequence of these morphological characteristics on rheology and conductivity is described below. For reasons that we will clarify, the dependence of morphology, mechanical properties, and ion transport of single-ion-conducting block copolymers on composition is qualitatively different from that of uncharged block copolymers outlined in the first paragraph of the Introduction.

EXPERIMENTAL SECTION

Block Copolymers. The syntheses of PEO-*b*-PSLiTFSI and PEO-*b*-P[$(STFSI)_2Mg$] block copolymers were described in prior work.[16−18] Briefly, a 9.5 kg mol^{-1} PEO macroinitiator was used to synthesize a series of PEO-*b*-PSKTFSI copolymer precursors. The potassium ion in each precursor was exchanged in separate reactions to yield a matched pair of PEO-*b*-PSLiTFSI and PEO-*b*-P[$(STFSI)_2Mg$] block copolymers. Following ion exchange, the water was sublimed under reduced pressure and 10 °C. Polymers were then further dried in a glovebox antechamber under vacuum at 90 °C for at least 12 h. Polymers were then brought into a glovebox for sample preparation. Polymerization was verified with ^1H NMR (Figure S1) and GPC (Figure S2), and ion exchange was verified via ICP-OES (inductively coupled plasma optical emission spectroscopy) (Figure S3).

Polymers are labeled PEO−PSLiTFSI(x−y) or PEO−P[$(STFSI)_2Mg$](x−y), where x and y are the molecular weights of the PEO and PSLiTFSI (or P[$(STFSI)_2Mg$]) blocks, respectively, in kg mol^{-1}. The resulting molecular weights (M_n), dispersities ($Đ$), ion concentrations (r), and volume fractions (ϕ) for the copolymers in this study are listed in Table 1. The volume fractions were estimated using the densities of PEO (1.12 g cm^{-1}), PSLiTFSI (1.57 g cm^{-1}), and P[$(STFSI)_2Mg$] (1.58 g cm^{-1}) homopolymers.[16,18] The ion concentration is quantified by r, where r = $[Li^+][EO]^{-1}$ for the PEO−PSLiTFSI copolymers and r = $[Mg^{2+}][EO]^{-1}$ for the magnesiated copolymers.

Differential Scanning Calorimetry. Polymer samples were hermetically sealed in aluminum pans inside an argon glovebox. Glovebox integrity was maintained during sample preparation. Experiments were carried out on a Thermal Advantage Q200 calorimeter at the Molecular Foundry (LBNL) in the following sequence: heating, cooling, heating. Each heating run was at a 20 °C

DOI: 10.1021/acs.macromol.7b01686
Macromolecules 2017, 50, 8765−8776

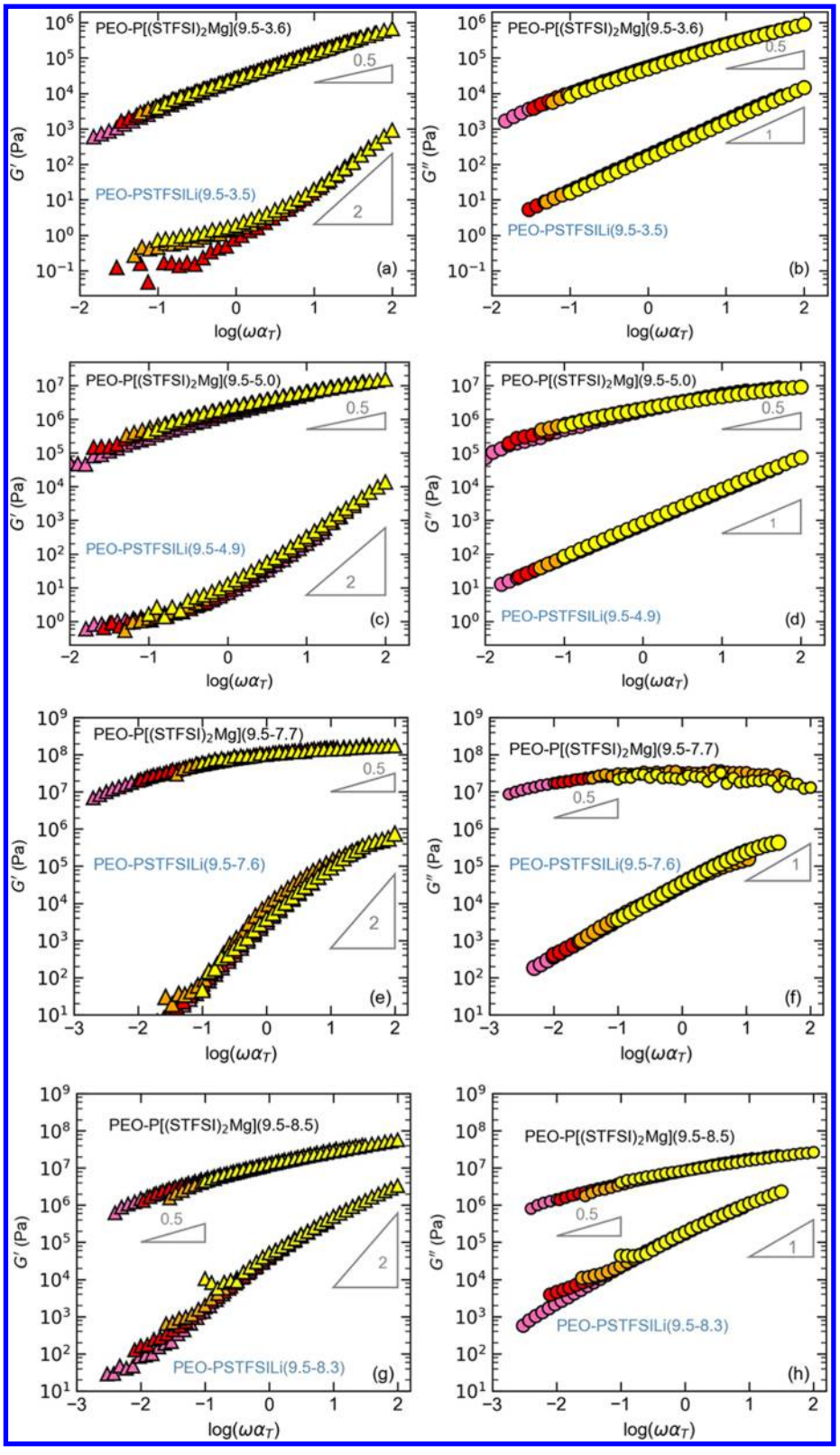

Figure 2. Master curves of G' and G'' of the matched copolymer pairs, where α_T is the shift factor as a function of reduced frequency at a reference temperature of 60 °C. PEO−PSLiTFSI(9.5−3.5) and P[$(STFSI)_2Mg$](9.5−3.6): (a) G', (b) G''; PEO−PSLiTFSI(9.5−4.9) and P[$(STFSI)_2Mg$]-(9.5−5.0): (c) G', (d) G''; PEO−PSLiTFSI(9.5−7.6) and P[$(STFSI)_2Mg$](9.5−7.7): (e) G', (f) G''; PEO−PSLiTFSI(9.5−8.3) and P[$(STFSI)_2Mg$](9.5−8.5): (g) G', (h) G''. The expected scalings for simple liquids ($G' \sim \omega^2$ and $G'' \sim \omega$) and ordered block copolymers ($G' \sim \omega^{0.5}$ and $G'' \sim \omega^{0.5}$) are shown in each figure.

min^{-1} rate, and the cooling run was conducted with a 2 °C min^{-1}. The temperature range was from −90 to 120 °C. The melting temperature and glass transition temperature were obtained from the second heating run.

DOI: 10.1021/acs.macromol.7b01686
Macromolecules 2017, 50, 8765−8776

Small-Angle X-ray Scattering. In an argon glovebox, samples were melt-pressed (60−90 °C) into AFLAS rubber spacers (800 μm thick) until translucent pucks were obtained. Samples were hermetically sealed in custom-made sample holders with Kapton windows. Samples were annealed overnight at 90 °C, and they were slowly cooled for 12 h to room temperature. Acquisitions of the magnesiated copolymers were conducted at the Stanford Synchrotron Radiation Lightsource (SSRL), and acquisitions of the lithiated copolymers were obtained at the Advanced Light Source (LBNL).[25] Glassy carbon (sample M13 provided by Jan Ilavsky) was used as the standard for absolute scattering.[26] The beam center and sample-to-detector distance were calibrated using silver behenate in Ilavsky's Nika module for Igor Pro.[27] The scattering profile of an empty sample holder was obtained as I_{air}. An empty sample holder with two Kapton films was used to acquire I_{Kapton}. The sample (I_{Sample}), I_{Kapton}, and I_{air} were all acquired with the same exposure time. The final scattering profiles were obtained by the following equation:

$$I_{corrected} = c \times \frac{I_{Sample} - I_{air} - \frac{T_{Sample}}{T_{Kapton}}(I_{Kapton} - I_{air})}{\text{sample thickness} \times \text{time}} \quad (1)$$

The scaling constant c for absolute intensity was obtained with the aid of Jan Ilavsky's Irena module in Igor Pro.[28] The transmission coefficients of the polymer sample and Kapton sample are T_{Sample} and T_{Kapton}, respectively.

Rheometry Experiments. A parallel-plate geometry was used on a Rheometric Scientific ARES (Advanced Rheometric Expansion System) rheometer. Rheometry measurements were conducted starting with 90 °C and cooled in 10 °C intervals until 50 °C. Thermal expansion of the plattens at each temperature was taken into account using a thermal expansion factor of 2.2 μm °C^{-1}. Samples were first subjected to a dynamic strain sweep test at 1 rad s^{-1} to determine a linear regime in which the storage (G') and loss (G'') moduli were constant as a function of strain. A strain in this linear regime was chosen such that the torque in the subsequent dynamic frequency sweep test was greater than 0.2 g·cm of force. The gap distance was adjusted for every temperature, as the polymer sample would contract with decreasing temperature. Final sample gap distances were between 0.5 and 1.5 mm.

All lithiated polymers were measured with 25 mm diameter plates, and the magnesiated copolymers were measured with 8 mm plates. A larger geometry was necessary for the lithiated copolymers because a higher strain was necessary to obtain strain-independent moduli. The PEO 9.5 kg mol^{-1} hompolymer was measured using a 50 mm plate geometry.

A 7.9 and 15.9 mm mold each made of fabric-reinforced silicone rubber sheet with an adhesive back (purchased from McMaster-Carr) was adhered onto a clean Teflon sheet. The magnesiated samples were melt-pressed into the 7.9 mm molds, and the lithiated copolymers were melted into the 15.9 mm molds. (The PEO 9.5 kg mol^{-1} homopolymer was prepared in a 25.4 mm mold.) The PEO homopolymer and lithiated samples were degassed under vacuum for 12 h at 90 °C to remove air bubbles. The magnesiated samples were pressed under 73 psi overnight at 90 °C for effective removal of air bubbles. The samples were then subjected to a slow cooling for 12 h under an inert atmosphere of nitrogen gas, and they were left at room temperature overnight for 12 h in an inert environment. The samples were then brought back into the glovebox for sample removal from the mold. The free-standing samples were removed from the glovebox in an airtight container for sample loading.

The plattens were rubbed clean with isopropanol before fixing them into the rheometer. An oven providing an inert atmosphere surrounded the plattens for the experiment. The plattens were heated up to 65 °C, at which point the gap was zeroed. The samples were quickly loaded concentrically to the plates at this temperature. The lithiated samples melted and thermally expanded, upon which the sample was pressed by the top plate until the sample filled up approximately 50% of the gap volume. Samples were then heated to 90 °C upon which samples thermally expanded to fill the gap volume. The samples were pressed with the top platten until the sample filled up the void space, and a slight polymer bulge was observed at the edges. Any residual polymer drip was removed, being careful not to damage the integrity of the polymer loaded in the plates. The robust magnesiated samples were pressed in the plattens until they filled the sample space. Samples equilibrated in the plattens for an hour before the start of the experiment. Samples were equilibrated for 20 min at every subsequent temperature before measurement.

Ionic Conductivity. Samples for ionic conductivity and measurement of the lithiated copolymers were reported in a previous publication.[16] Ionic conductivity samples of the magnesiated copolymers differed only in that they utilized more physically robust spacers, Garolite 10 (McMaster-Carr). Samples were approximately 100−200 μm thick.

RESULTS AND DISCUSSION

The frequency (ω) dependence of G' and G'' was measured for all polymers between 60 and 90 °C. These data are shown in Figures S5−S12. Time−temperature superposition (TTS) was used to generate master curves, and the results are shown in Figure 2. Figures 2a and 2b show G' and G'' against reduced frequency for the matched pair: PEO−P[(STFSI)$_2$Mg](9.5-3.6) and PEO−PSLiTFSI(9.5-3.5). For the lithiated copolymer, $G'' > G'$ and $G'' \sim \omega$ over the entire frequency range. These are characteristics of viscoelastic liquids. In the range $1 < \log(\omega\alpha_T) < 2$, $G' \sim \omega^2$; α_T is the shift factor used at temperature, T. The G' versus ω scaling observed in this frequency window is also characteristic of viscoelastic liquids. The liquid-like rheological properties of PEO−PSLiTFSI(9.5−3.5) are consistent with our previous studies, indicating that these copolymers are disordered.[16,17] However, in the low-frequency regime, $\log(\omega\alpha_T) < 0$, we observe deviations from rheological liquid-like behavior in PEO−PSLiTFSI(9.5−3.5); G' approaches a frequency-independent plateau. This plateau may arise from physical cross-links due to the presence of widely spaced ionic clusters.[29−31] The rheological data suggest that these clusters have a lifetime of 10−100 s at 60 °C. Uncharged block copolymers in the disordered state do not exhibit such a plateau.[6] The rheological properties of PEO−P[(STFSI)$_2$Mg]-(9.5−3.6) differ qualitatively from those of the lithiated matched pair (Figure 2a and 2b). Over the accessible reduced frequency range, G' of the magnesiated sample at a given reduced frequency is 3−4 orders of magnitude higher than its lithiated counterpart. Similarly, G'' is 2−3 orders of magnitude higher than its lithiated counterpart. In addition, both G' and G'' of the magnesiated sample are similar in magnitude and scale with $\omega^{0.5}$ across much of the accessible reduced frequency window. These characteristics are often seen in microphase-separated block copolymers.[6,32]

The rheological properties of the matched pair PEO−P[(STFSI)$_2$Mg](9.5−5.0) and PEO−PSLiTFSI(9.5−4.9) (Figures 2c and 2d) are similar to those described in the preceding paragraph. Further increase of the molecular weight of the ion-containing block to 7.7 kg mol^{-1} results in qualitative differences (Figures 2e and 2f). At high frequency, we see deviations from liquid-like behavior that are not present in the lithiated samples discussed in the previous paragraph. In particular, we see beginnings of glassy response at high frequency. We attribute this to the increase in the volume fraction of the glassy PSLiTFSI block. Low-frequency deviations from liquid-like rheological behavior in PEO−PSLiTFSI(9.5−7.6) are no longer evident. While there are many possible explanations for this, it is likely that this is due to the limited frequency window; the low-frequency plateau and

DOI: 10.1021/acs.macromol.7b01686
Macromolecules 2017, 50, 8765−8776

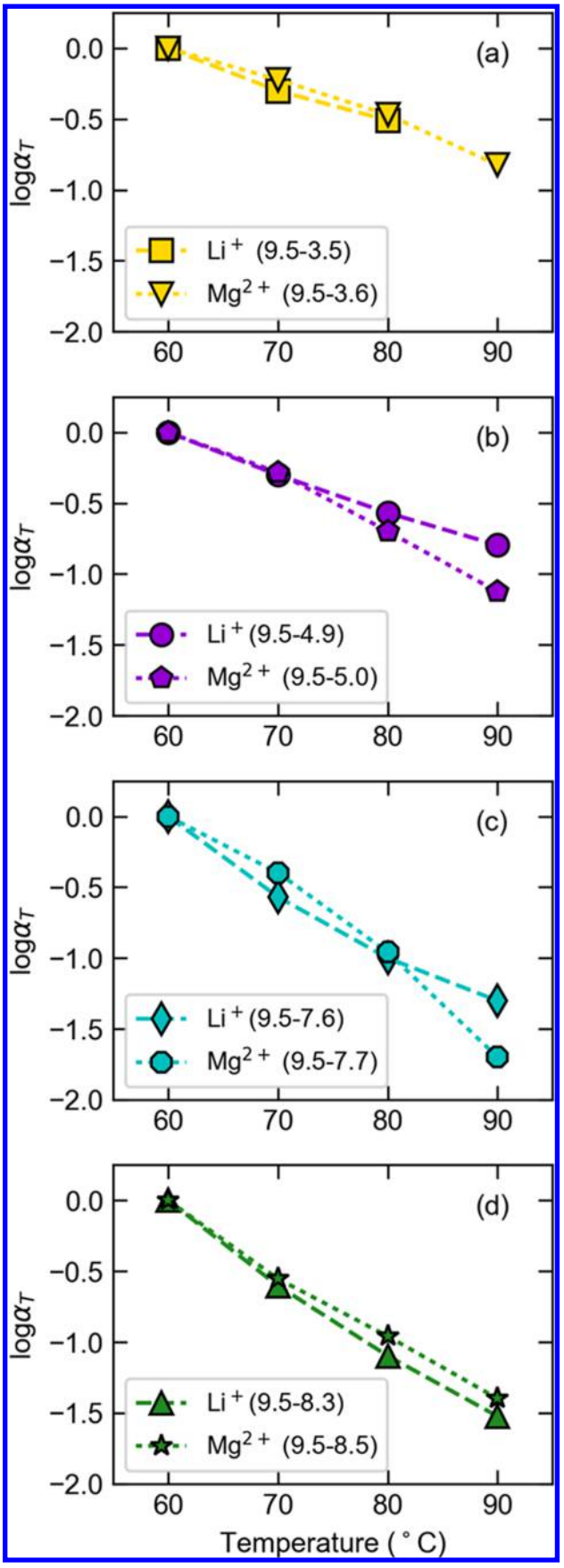

Figure 3. Shift factors for the matched copolymer pairs as a function of temperature.

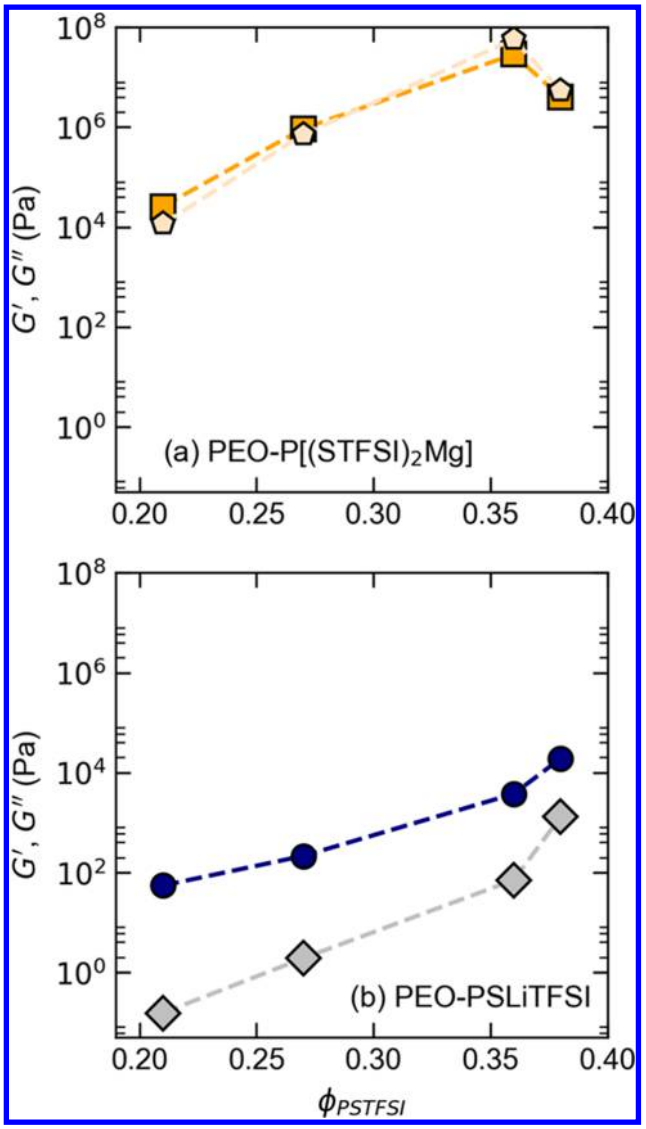

Figure 4. G' and G'' at 80 °C and ω = 1 rad s^{-1} plotted against the volume fraction of the ion-containing block, ϕ_{PSTFSI}, of (a) G' (orange squares) and G'' (peach pentagons) of the magnesiated copolymers and (b) G' (gray diamonds) and G'' (navy circles) of the lithiated copolymers.

glassy modes occur at reduced frequencies outside our experimental window. We also note the presence of high-frequency glassy plateaus in both G' and G'' of PEO−P[(STFSI)$_2$Mg](9.5−7.7). The rheological properties of the PEO−P[(STFSI)$_2$Mg](9.5−8.5) and PEO−PSLiTFSI(9.5−8.3) matched pair are shown in Figures 2g and 2h. The liquid-like terminal regime is not seen in PEO−PSLiTFSI(9.5−8.3). We posit that the increase in the volume fraction of the glassy component results in the emergence of glassy dynamics in the accessible frequency window. Interestingly, the glassy plateau evident in PEO−P[(STFSI)$_2$Mg](9.5−7.7) is not seen in PEO−P[(STFSI)$_2$Mg](9.5−8.5). We will explain this behavior shortly.

The temperature dependence of shift factors for each matched pair is shown in Figure 3, where log(α_T) is plotted versus temperature. The surprising observation is that the shift factors for the lithiated and magnesiated matched pairs at a given temperature are very similar in spite of the fact that their rheological properties are very different. For example, at

DOI: 10.1021/acs.macromol.7b01686
Macromolecules 2017, 50, 8765−8776

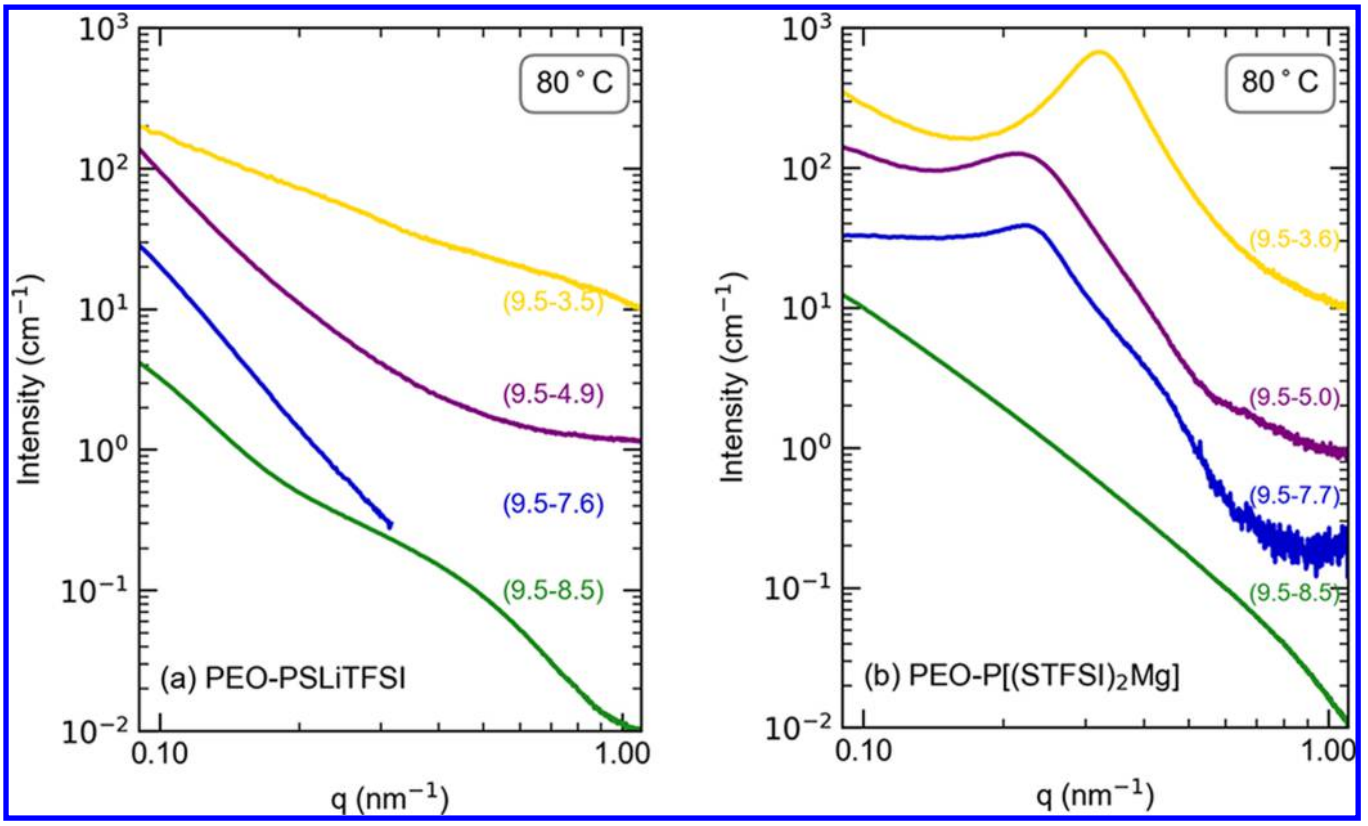

Figure 5. SAXS scattering intensity versus the magnitude of the scattering vector, q. (a) SAXS profiles of the lithiated block copolymers. The top profile in yellow is PEO−PSLiTFSI(9.5−3.5). The second profile from the top in purple is PEO−PSLiTFSI(9.5−4.9). The third profile in blue is PEO−PSLiTFSI(9.5−7.6). The bottom-most profile is PEO−PSLiTFSI(9.5−8.3) in green. The profiles are vertically offset by factors of 600, 25, 15, and 1. (b) SAXS profiles of the matched magnesiated block copolymers in the same order and color coordination. The scattering profiles are vertically offset for clarity by factors of 150, 20, 15, and 0.2, respectively.

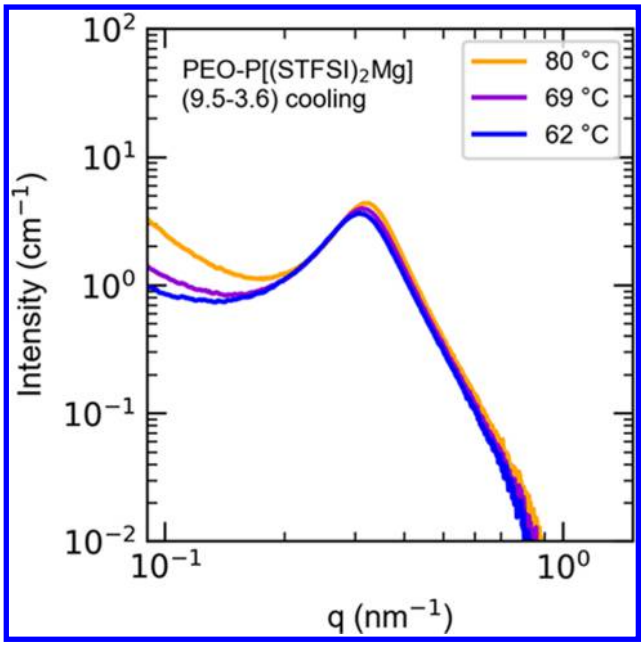

Figure 6. Cooling SAXS profiles for PEO−P[(STFSI)$_2$Mg](9.5−3.6).

$\log(\omega\alpha_T) = -1$, the G' of PEO−P[(STFSI)$_2$Mg](9.5−7.7) is 6 orders of magnitude larger than its lithiated matched pair (Figures 2e and 2f). In comparison, the differences in the shift factors of these two systems are unremarkable (Figure 3c). The same can be said of all of the data in Figures 2 and 3.

In principle, time−temperature superposition (TTS) applies to thermorheologically simple polymers, typically homopolymers.[33] While the data in Figures 2 and 3 are limited to temperatures above both the crystallization and glass transition temperatures of the samples, further work is needed to ascertain the extent to which TTS is applicable to single-ion-conducting block copolymers.

In Figure 4a, we plot G' and G'' (as measured, unshifted) of each of the magnesiated copolymers at fixed temperature and frequency (80 °C and ω = 1 rad s^{-1}) versus ϕ_{PSTFSI}. Both G' and G'' increase steadily with increasing ϕ_{PSTFSI} (or equivalently with increasing molecular weight of the ion-containing block), until ϕ_{PSTFSI} reaches a threshold of 0.36. Beyond this threshold, both G' and G'' decrease. In Figure 4b, we plot G' and G'' of each of the lithiated copolymers at fixed temperature and frequency (80 °C and ω = 1 rad s^{-1}) versus ϕ_{PSTFSI} of that sample. In this set, both G' and G'' increase steadily with increasing ϕ_{PSTFSI} across the entire experimental window. (While we have shown rheology data at a particular temperature and frequency in Figure 4, the same conclusion is obtained for data at all temperatures and frequencies.) To explain the distinct trends in the rheological features of the lithiated and magnesiated copolymer systems, we conducted SAXS experiments.

The SAXS profiles obtained at 80 °C for each of the copolymers are shown in Figure 5, where the scattering intensity, I, is plotted against the magnitude of the scattering vector, q. The scattering profiles of the lithiated copolymers are shown in Figure 5a. The scattering from these samples was

DOI: 10.1021/acs.macromol.7b01686
Macromolecules 2017, 50, 8765−8776

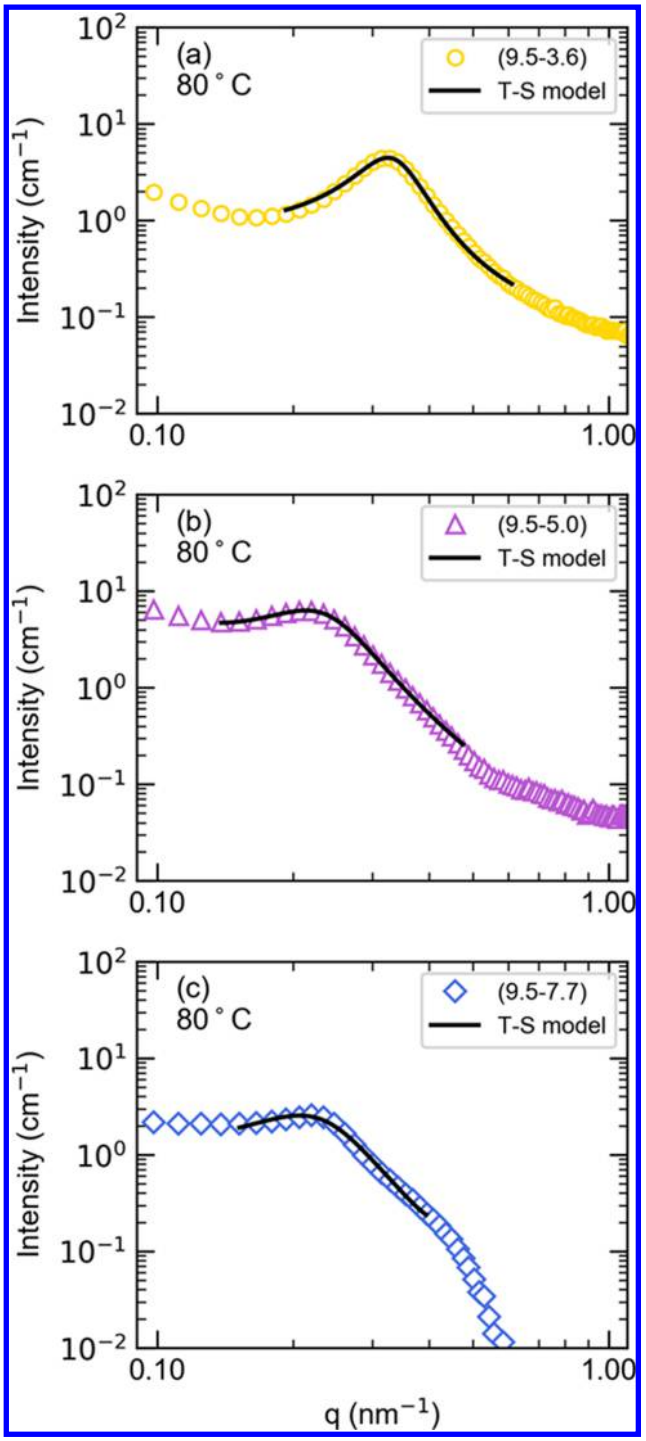

Figure 7. SAXS intensity graphed against the magnitude of the scattering vector, q, for the three microphase-separated magnesiated copolymers at 80 °C. For clarity, every 10th data point is shown by a shape. The solid black lines are the T−S model fits to the data.

comparable to the scattering from the empty cell. In one of the samples (PEO−PSLiTFSI(9.5−7.6)) the data are truncated because the measured scattering from the sample fell below that of the empty cell at $q > 0.32$. We conclude that all of the PEO−PSLiTFSI samples are completely disordered (homogeneous). This is consistent with our previous work wherein we concluded that the effective Flory−Huggins interaction parameter, χ, between PEO and PSLiTFSI is negative.[18]

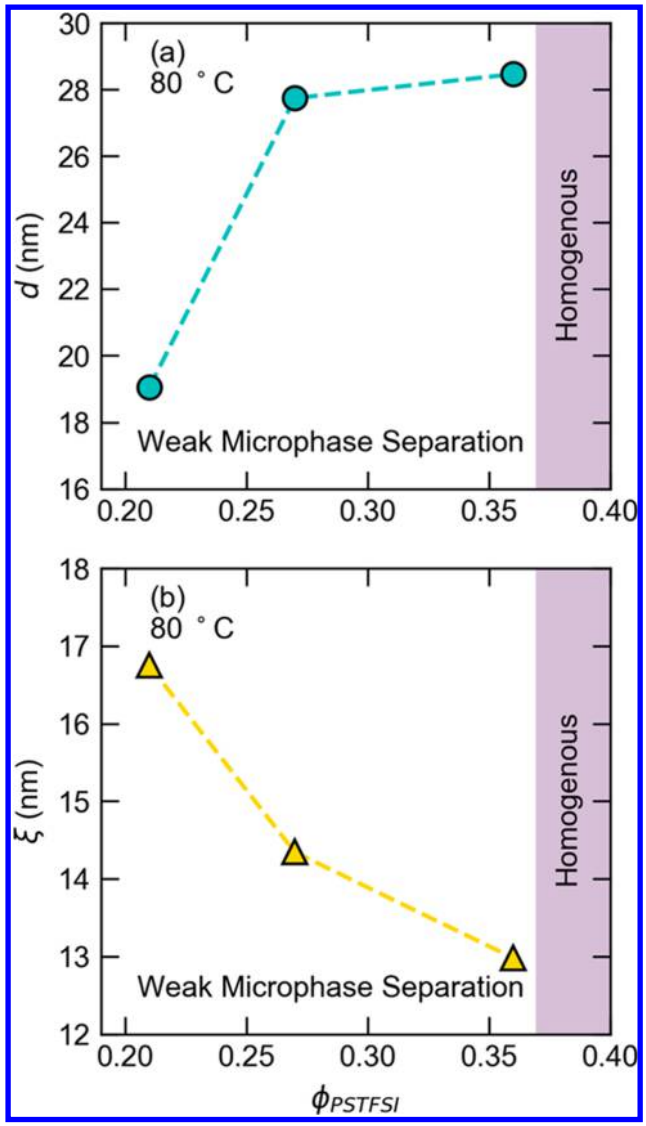

Figure 8. Results of T−S fits at 80 °C for the magnesiated samples: (a) d, in blue circles, and (b) ξ, in yellow triangles, versus ϕ_{PSTFSI}.

The scattering profiles of the magnesiated copolymers are shown in Figure 5b. Sample PEO−P[(STFSI)$_2$Mg](9.5−3.6) with $\phi_{PSTFSI} = 0.21$ exhibits a broad well-defined peak at $q = q^* = 0.330$ nm^{-1}. In addition, we see an upturn at low q. We take the presence of scattering peaks to be a signature of microphase separation. As we increase ϕ_{PSTFSI} to 0.27 (PEO−P[(STFSI)$_2$Mg](9.5−5.0)), a broad peak is also observed at $q^* = 0.227$ nm^{-1}. This peak is not as well-defined as the sample with $\phi_{PSTFSI} = 0.21$. Further increase of ϕ_{PSTFSI} to 0.36 results in a very weak scattering maximum at $q^* = 0.221$ nm^{-1}. Finally, increasing ϕ_{PSTFSI} to 0.38 results in a monotonic scattering profile with no evidence of a scattering maximum. As mentioned in the Introduction, the tendency for ordering in uncharged block copolymers is expected to increase with increasing molecular weight of the minor component when the chain length of the major component is held fixed. The data in Figure 5b are not in accordance with this expectation. The data presented here do not allow for distinction between weak microphase separation and disordered concentration fluctuations; we use the term weak microphase separation in the discussion below.

DOI: 10.1021/acs.macromol.7b01686
Macromolecules 2017, 50, 8765−8776

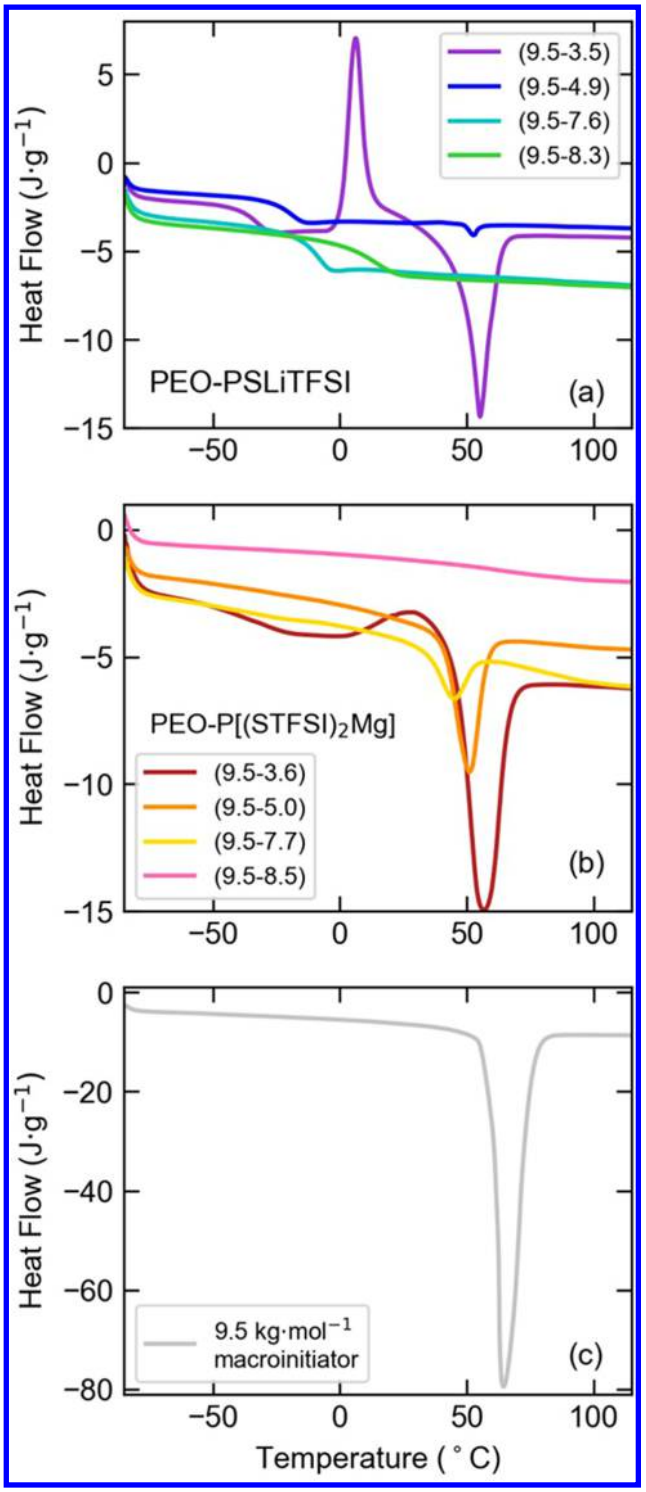

Figure 9. DSC thermograms of (a) the lithiated copolymers, the (b) magnesiated copolymers, and (c) the PEO 9.5 kg mol^{-1} homopolymer.

The low-angle SAXS scattering seen in Figure 5b at $q < 0.2$ nm^{-1} is inconsistent with the expected scattering from both disordered and microphase-separated uncharged block copolymers. In Figure 6 we show the temperature dependence of $I(q)$ of PEO−P[(STFSI)$_2$Mg](9.5−3.6). It is evident that the low q scattering decreases considerably when the sample is cooled to 62 °C. The changes in low q scattering are reversible.

The scattering profiles from weakly microphase-separated magnesiated block copolymers are qualitatively different from those of uncharged block copolymers. Features like low-angle upturns have previously been observed in charged block copolymers.[34] Such features may be related to the fact that our samples are not perfectly monodisperse; small differences in the length of the charged block may lead to the formation of large length-scale structures with low-angle scattering signatures. The SAXS profiles of the weakly microphase-separated magnesiated block copolymers (Figure 5b) are qualitatively consistent with a model proposed by Teubner and Strey.[35] This model (T−S model) was originally developed to describe scattering from oil/water/surfactant microemulsions.[35−37] It assumes a sinusoidal correlation function with a characteristic period d that is exponentially damped with characteristic correlation length, ξ. Our objective is to describe the morphology of the weakly microphase-separated magnesiated block copolymers using these parameters.

The T−S equation for the scattering intensity is described by eq 2, where the additional term, I_{bgd}, accounts for the connectivity of polymer chains.[7,35,38−40]

$$I(q) = \frac{1}{a + bq^2 + cq^4} + I_{bgd}(q) \quad (2)$$

$$I_{bgd}(q) = \frac{1}{eq^2 + g} \quad (3)$$

From the fitting coefficients (a, b, and c), one can determine the correlation length (ξ) and the domain spacing (d), given by eqs 4 and 5.

$$\xi = \left[\frac{1}{2}\left(\frac{a}{c}\right)^{1/2} + \frac{b}{4c}\right]^{-1/2} \quad (4)$$

$$d = 2\pi\left[\frac{1}{2}\left(\frac{a}{c}\right)^{1/2} - \frac{b}{4c}\right]^{-1/2} \quad (5)$$

In Figure 7, we show a least-squares fit to the T−S equation for the microphase-separated magnesiated copolymers at 80 °C. It is evident that the shape of the main scattering peak in our samples is consistent with the T−S equation. (Analyzing features like the low-angle upturn requires more sophisticated models.) In Figure 8, we show d and ξ, obtained from the T−S fits as a function of ϕ_{PSTFSI}. We find that d increases with increasing ϕ_{PSTFSI} (Figure 8a). This is attributed to the increase in chain length with increasing ϕ_{PSTFSI}. In contrast, ξ decreases with increasing ϕ_{PSTFSI} (Figure 8b), reflecting the decreasing tendency for microphase separation. Note that at $\phi_{PSTFSI} = 0.38$ no microphase separation is observed in the magnesiated sample. The decrease in ξ and homogenization with increasing ϕ_{PSTFSI} is qualitatively different from the behavior of uncharged block copolymers. We posit that this observation is due to the favorable interactions between Mg^{2+} and PEO. Above a critical value of $\phi_{PSTFSI} = 0.36$, the Mg^{2+} ions prefer to be solvated in the PEO microphase. The analogous critical value of the ϕ_{PSTFSI} of the lithiated chains is much smaller. We attribute this to two factors: (1) the interactions between ether oxygens and Li^+ are more favorable than those between the ether oxygens and Mg^{2+}, and (2) the divalent nature of Mg^{2+} increases the tendency for these ions to be localized in the PSTFSI block. It should be noted that this is the first report of homogenization in magnesiated single-ion-conducting block copolymers.

DOI: 10.1021/acs.macromol.7b01686
Macromolecules 2017, 50, 8765−8776

Table 2. Summary of DSC Experiments[a]

	w_{PEO}	$T_{m,PEO}$ (°C)	$\Delta H_{m,PEO}$ (J/g)	$X_{c,PEO}$ (%)	T_g (°C)
PEO 9.5	1	59.7	113	55	n.o.
PEO−PSLiTFSI(9.5−3.5)	0.73	48.9	82	40.	−33.1
PEO−PSLiTFSI(9.5−4.9)	0.66	50.6	0.42	0.20	−15.3
PEO−PSLiTFSI(9.5−7.6)	0.56	n.o.	n.o.	n.o.	−7.98
PEO−PSLiTFSI(9.5−8.3)	0.53	n.o.	n.o.	n.o.	14.1
PEO−P[(STFSI)$_2$Mg(9.5−3.6)]	0.73	44.8	67	32	−26.2
PEO−P[(STFSI)$_2$Mg(9.5−5.0)]	0.66	46.6	36	17	2.31
PEO−P[(STFSI)$_2$Mg(9.5−7.7)]	0.55	35.0	12	5.6	16.2
PEO−P[(STFSI)$_2$Mg(9.5−8.5)]	0.53	n.o.	n.o.	n.o.	59.5

[a]The weight fraction of PEO (w_{PEO}), the (onset) melting temperature (T_m), melting enthalpy normalized by PEO weight fraction ($\Delta H_{m,PEO}$), degree of crystallinity ($X_{c,PEO}$), and the glass transition temperature (T_g) are listed. n.o. = not observed.

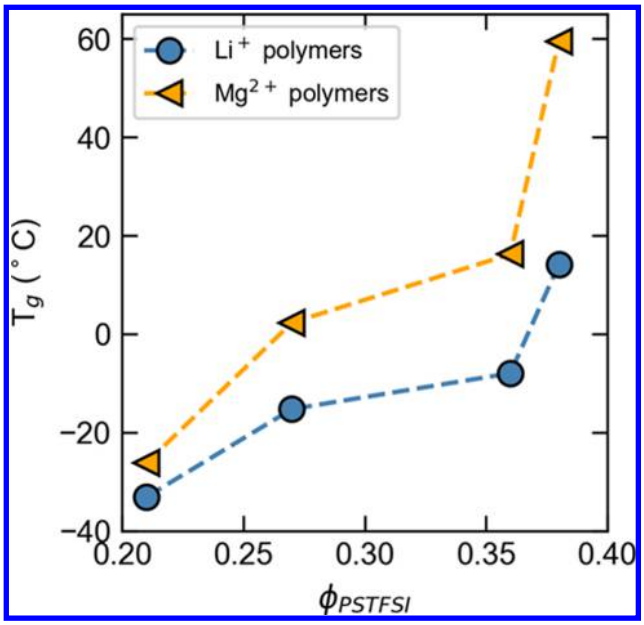

Figure 10. Graph of the glass transition temperature, T_g, plotted against the volume fraction, ϕ_{PSTFSI}, of the PSLiTFSI or P-[(STFSI)$_2$Mg] block. The blue circles represent data for the lithiated copolymers, and the orange triangles correspond to the magnesiated copolymers.

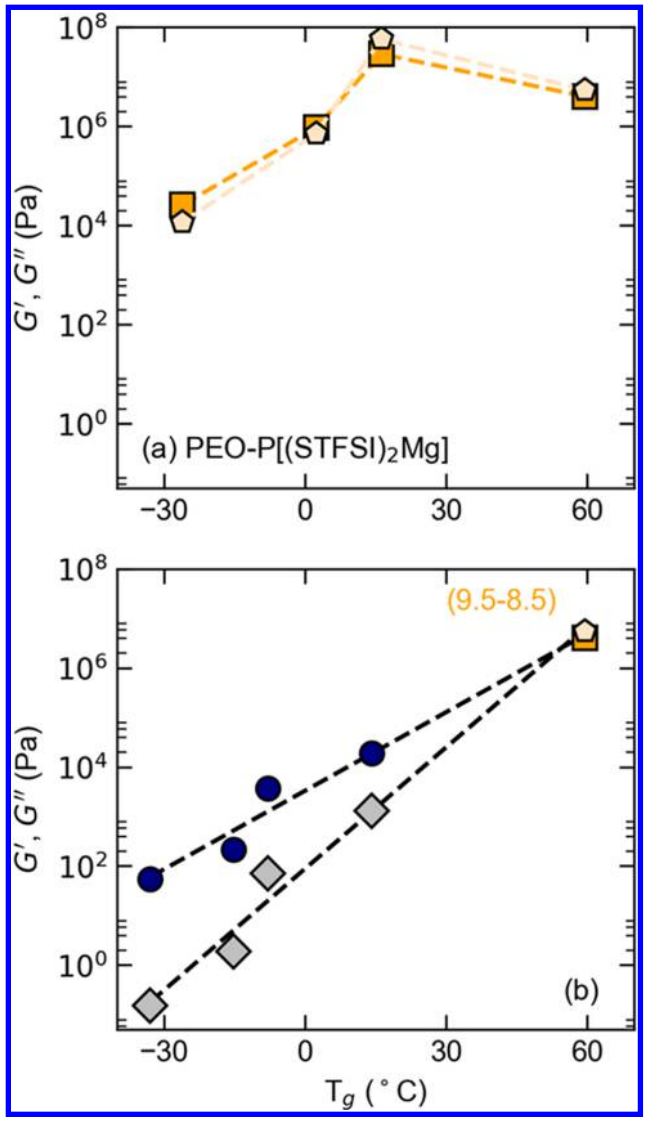

Figure 11. G' and G'' at 80 °C and ω = 1 rad s^{-1} plotted against T_g of each sample (a) G' (orange squares) and G'' (peach pentagons) of the magnesiated copolymers and (b) G' (gray diamonds) and G'' (navy circles) of the lithiated copolymers with PEO−P[(STFSI)$_2$Mg](9.5−8.5) data.

The main objective of this paper is to discuss the properties of our copolymers above the melting point of the PEO block; all of the data in Figures 2−8 are in this regime. The melting point of PEO homopolymers is in the vicinity of 60 °C.[41] In many cases this crystallization drives microphase separation in our single-ion-conducting block copolymers.[16−18] This is shown in Figure 9, where DSC data from our polymers are shown. PEO−PSLiTFSI(9.5−3.5) and -(9.5−4.9) exhibit a readily identifiable melting temperature, T_m, while PEO−PSLiTFSI(9.5−7.6) and -(9.5−8.3) did not show signatures of crystallinity. (PEO−PSLiTFSI(9.5−3.5) exhibits a crystallization peak prior to melting, as is often seen in semicrystalline polymers.[42,43]) The absence of crystallinity is due to the migration of the Li$^+$ ions from the PSTFSI block to the PEO block.[16,17] Similarly, the magnesiated copolymers, PEO−P[(STFSI)$_2$Mg](9.5−3.6), -(9.5−5.0), and -(9.5−7.7), exhibited melting behavior (Figure 9b) while PEO−P-[(STFSI)$_2$Mg](9.5−8.5) did not. As argued above, the absence of crystallinity in this case is due to the migration of Mg^{2+} ions from the PSTFSI block to the PEO block. The melting behaviors of our samples are summarized in Table 2, where we list T_m, the melting enthalpy, ΔH_m, and degree of crystallinity, X_c. We calculate the degree of crystallinity (X_c) from eq 6, where ΔH_m^0 is the melting enthalpy of a fully crystalline PEO

DOI: 10.1021/acs.macromol.7b01686
Macromolecules 2017, 50, 8765−8776

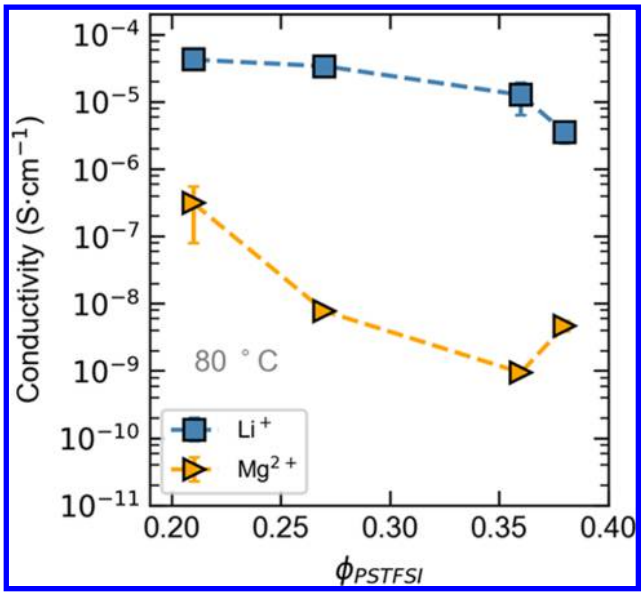

Figure 12. Ionic conductivity plotted against ϕ_{PSTFSI} at 80 °C of the lithiated copolymers (blue squares) and the magnesiated copolymers (orange triangles).

sample (206 J g^{-1}) and w_{PEO} is the PEO weight fraction of the copolymer.[43,44]

$$X_c = \frac{\Delta H_m}{\Delta H_m^0 w_{PEO}} \quad (6)$$

It is evident that X_c is highly dependent on ϕ_{PSTFSI} (Table 2).

The DSC scans also contain signatures of a glass transition temperature, T_g, and these values are also listed in Table 2 and plotted in Figure 10. Increasing the molecular weight of the ion-containing block results in an increase in T_g. This is not surprising because the ion-containing blocks are known to be glassy.[11] Within each matched pair, the T_g of the magnesiated copolymer is higher. Comparing data obtained from the matched pair with the highest ϕ_{PSTFSI} = 0.38, we conclude that the presence of divalent Mg^{2+} ions retards segmental motion to a greater extent than univalent Li^+ ions (Figure 10). While the same qualitative conclusion may be drawn from other matched pairs, the difference in morphology precludes quantitative comparisons. The difference in T_g increases with increasing volume fraction of the ion-containing block from 7 to 46 °C.

In Figure 11a, we plot G' and G'' (as measured, unshifted) of each of the magnesiated copolymers at fixed temperature and frequency (80 °C and ω = 1 rad s^{-1}) versus T_g of that sample. Both G' and G'' increase steadily with increasing T_g (or equivalently with increasing molecular weight of the ion-containing block, see Figure 10), until T_g reaches a threshold of 16 °C. Beyond this threshold, both G' and G'' decrease in spite of the fact that T_g increases. The reason for this is now obvious: PEO−P[(STFSI)$_2$Mg](9.5−8.5) is homogeneous while the other magnesiated copolymers are weakly microphase separated.

In Figure 11b, we plot G' and G'' of each of the lithiated copolymers at fixed temperature and frequency (80 °C and ω = 1 rad s^{-1}) versus T_g of that sample. In this set, both G' and G'' increase steadily with increasing T_g across the entire experimental window. The reason for this is also obvious; all of the lithiated samples are homogeneous. Also shown in Figure 11b is the data for PEO−P[(STFSI)$_2$Mg](9.5−8.5). Surprisingly, data from the lithiated copolymers and PEO−P[(STFSI)$_2$Mg](9.5−8.5) fall on the same line (see dashed lines in Figure 11b). (While we have shown rheology data at a particular temperature and frequency in Figure 11, the same conclusion is obtained for data at all temperatures and frequencies.) It is thus evident that the sheer moduli of both lithiated and magnesiated block copolymers that are homogeneous are mainly governed by T_g.

In Figure 12, we compare the ionic conductivity of the block copolymer electrolytes at 80 °C. Within each matched pair, the ionic conductivity of the magnesiated block copolymer is 2−4 orders of magnitude lower than that of its lithiated counterpart. This is consistent with previous studies on lower molecular weight lithiated and magnesiated single-ion-conducting copolymers. These ionic conductivities were on the order of 10^{-5} and 10^{-6} S cm^{-1} at 80 °C for the lithiated and magnesiated copolymers, respectively.[18] Target values for single-ion conductors for electric vehicle application is 10^{-4} S cm^{-1}. The conductivity of the lithiated copolymers decreases smoothly with increasing ϕ_{PSTFSI} (Figure 12). This can be attributed to increasing T_g. The conductivity trend of the magnesiated copolymers is different. The conductivity decreases with increasing ϕ_{PSTFSI} in the range 0.21 ≤ ϕ_{PSTFSI} ≤ 0.36; this can also be attributed to increasing T_g. However, there is a sudden increase in conductivity by a factor of 3 when ϕ_{PSTFSI} is increased from 0.36 to 0.38. The reason for this is clear: conductivity is higher when the copolymer is homogeneous, as the magnesium ions are in contact with mobile PEO segments. This is the first reported measurement of conductivity in disordered magnesiated single-ion-conducting copolymer electrolytes.

CONCLUSION

We synthesized and characterized a series of matched pairs of lithiated and magnesiated single-ion-conducting block copolymer electrolytes. We used rheology, SAXS, DSC, and AC impedance spectroscopy to characterize our samples. We obtained master curves from the rheology measurements. At a given frequency and temperature, G' and G'' of the magnesiated copolymers were approximately 3−4 orders of magnitude higher than its lithiated matched pair. Furthermore, the lithiated copolymers showed liquid-like rheological signatures while the magnesiated samples did not. In spite of these differences, the shift factors for the matched copolymer pairs at a given temperature were similar. G' and G'' of the lithiated copolymers monotonically increased with ϕ_{PSTFSI}. This is expected due to the glassy nature of the ion-containing block. The magnesiated copolymers however followed a slightly different trend. While G' and G'' values increased with increasing ϕ_{PSTFSI} in the range 0.21 ≤ ϕ_{PSTFSI} ≤ 0.36, the modulus of the sample with ϕ_{PSTFSI} = 0.38 was lower than that of the sample with ϕ_{PSTFSI} = 0.36.

SAXS data showed that all of the lithiated samples were homogeneous. In contrast, the magnesiated samples with 0.21 ≤ ϕ_{PSTFSI} ≤ 0.36 were weakly microphase separated while the sample with ϕ_{PSTFSI} = 0.38 was homogeneous. Microphase separation is suppressed by increasing ϕ_{PSTFSI}, a trend that is qualitatively different than that seen in uncharged block copolymers. Homogenization is driven by favorable interactions between the ions and ether oxygens in the PEO block. The extent to which these interactions are captured by current models of microphase separation in charged polymers is unclear.[20,21] These favorable interactions are more dominant in

DOI: 10.1021/acs.macromol.7b01686
Macromolecules 2017, 50, 8765−8776

the lithiated samples. DSC data enabled determination of the crystallinity of the samples and T_g. Crystallinity is also dominated by interactions between ions and ether oxygens. Both T_g and the morphology affect G' and G'' of the lithiated and magnesiated copolymers. When the copolymers are completely disordered (Figure 11b), the shear moduli of both lithiated and magnesiated copolymers steadily increase with T_g. When the copolymers are weakly microphase separated, they follow a separate trend with T_g (Figure 11a). Similarly, the effects of T_g and morphology dictate the ionic conductivity.

■ ASSOCIATED CONTENT

Supporting Information

The Supporting Information is available free of charge on the ACS Publications website at DOI: 10.1021/acs.macromol.7b01686.

H NMR of block copolymers; GPC traces of the copolymers; ICP-OES of the lithiated and magnesiated copolymers; Teubner−Strey fitting parameters of the magnesiated copolymers at elevated temperatures; frequency-dependent shear moduli of the lithiated and magnesiated copolymers and PEO homopolymer (PDF)

■ AUTHOR INFORMATION

Corresponding Author

*E-mail nbalsara@berkeley.edu, phone (510) 642-8937 (N.P.B.).

ORCID

Adriana A. Rojas: 0000-0002-5587-6822

Nitash P. Balsara: 0000-0002-0106-5565

Notes

The authors declare no competing financial interest.

■ ACKNOWLEDGMENTS

This work was supported as part of the Joint Center for Energy Storage Research, an Energy Innovation Hub funded by the U.S. Department of Energy, Office of Science, Basic Energy Sciences. SAXS experiments were performed at the Lawrence Berkeley National Laboratory (LBNL) Advance Light Source, Beamline 7.3.3, supported by the Director of the Office of Science, Office of Basic Energy Sciences, of the U.S. Department of Energy under Contract DE-AC02-05CH11231. Use of the Stanford Synchrotron Radiation Lightsource, SLAC National Accelerator Laboratory, is supported by the U.S. Department of Energy, Office of Science, Office of Basic Energy Sciences, under Contract DE-AC02-76SF00515. We acknowledge Eric Schaible, Chenhui Zhu, and Christopher Tassone for beamline support. Work at the Molecular Foundry was supported by the Office of Science, Office of Basic Energy Sciences, of the U.S. Department of Energy under Contract DE-AC02-05CH11231.

■ NOMENCLATURE

PEO poly(ethylene oxide)

PEO-*b*-PSLiTFSI or PEO-PSLiTFSI poly(ethylene oxide)-*b*-polystyrenesulfonyllithium (trifluoromethyl sulfonyl) imide

PEO-*b*-P[(STFSI)$_2$Mg] or PEO-P[(STFSI)$_2$Mg] poly(ethylene oxide)-*b*-polystyrene-sulfonyl magnesium (trifluoromethyl sulfonyl) imide

SAXS small-angle X-ray scattering

Symbols

d the domain spacing

$Đ$ the dispersity

G' storage modulus

G'' loss modulus

ΔH_m the melting enthalpy

ΔH_m^0 the reference melting enthalpy

q magnitude of the scattering vector

I the scattering intensity

M_{PEO} molecular weight of the PEO block

$M_{PSLiTFSI}$ molecular weight of the PSLiTFSI block

T_{SAMPLE} transmission coefficient of the sample

T_c the crystallization temperature

T_g the glass transition temperature

T_m the onset melting temperature

w_{PEO} the weight fraction of PEO

Greeks

α_T shift factor

ξ correlation length

π pi

ϕ_{PEO} volume fraction of the PEO block

ϕ_{PSTFSI} volume fraction of the ion-containing block

ω frequency

■ REFERENCES

(1) Leibler, L. Theory of Microphase Separation in Block Copolymers. *Macromolecules* **1980**, *13*, 1602−1617.

(2) Fredrickson, G. H.; Helfand, E. Fluctuation Effects in the Theory of Microphase Separation in Block Copolymers. *J. Chem. Phys.* **1987**, *87*, 697.

(3) Bates, F. S. Block Copolymer Thermodynamics: Theory and Experiment. *Annu. Rev. Phys. Chem.* **1990**, *41*, 525−557.

(4) Matsen, M. W.; Bates, F. Block Copolymer Microstructures in the Intermediate-Segregation Regime. *J. Chem. Phys.* **1997**, *106*, 2436.

(5) Matsen, M. W.; Schick, M. Stable and Unstable Phases of a Diblock Copolymer Melt. *Phys. Rev. Lett.* **1994**, *72*, 2660.

(6) Rosedale, J. H.; Bates, F. S. Rheology of Ordered and Disordered Symmetric Poly(ethylenepropy1ene)-Poly(ethylethy1ene) Diblock Copolymers. *Macromolecules* **1990**, *23*, 2329−2338.

(7) Morkved, T. L.; Stepanek, P.; Krishnan, K.; Bates, F. S.; Lodge, T. L. Static and Dynamic Scattering from Ternary Polymer Blends:Bicontinuous Microemulsions, Lifshitz lines, and Amphiphilicity. *J. Chem. Phys.* **2001**, *114*, 7247.

(8) Bates, F. S.; Rosedale, J. H.; Fredrickson, G. H. Fluctuation Effects in a Symmetric Diblock Copolymer Near the Order-Disorder Transition. *J. Chem. Phys.* **1990**, *92*, 6255.

(9) Almdal, K.; Bates, F. S.; Mortensen, K. Order, Disorder, and Fluctuation Effects in an Asymmetric Poly(ethylene-propylene)-poly(ethylethylene) Diblock Copolymer. *J. Chem. Phys.* **1992**, *96*, 9122.

(10) Hickey, R. J.; Gillard, T. M.; Lodge, T. P.; Bates, F. S. Influence of Composition Fluctuations on the Linear Viscoelastic Properties of Symmetric Diblock Copolymers near the Order-Disorder Transition. *ACS Macro Lett.* **2015**, *4*, 260−265.

(11) Bouchet, R.; Maria, S.; Meziane, R.; Aboulaich, A.; Lienafa, L.; Bonnet, J. P.; Phan, T. N. T.; Bertin, D.; Gigmes, D.; Devaux, D.; Denoyel, R.; Armand, M. Single-ion BAB triblock Copolymers as Highly Efficient Electrolytes for Lithium-Metal Batteries. *Nat. Mater.* **2013**, *12*, 452.

(12) Ryu, S.; Trapa, P. E.; Olugebefola, S. C.; Gonzalez-Leon, J. A.; Sadoway, D. R.; Mayes, A. M. Effect of Counter Ion Placement on Conductivity in Single-Ion Conducting Block Copolymer Electrolytes. J. of the. *J. Electrochem. Soc.* **2005**, *152*, A158−A163.

(13) Sadoway, D. R.; Huang, B.; Trapa, P. E.; Soo, P. P.; Bannerjee, P.; Mayes, A. M. Self-Doped Block Copolymer Electrolytes for Solid-

DOI: 10.1021/acs.macromol.7b01686
Macromolecules 2017, 50, 8765−8776

State, Rechargeable Lithium Batteries. *J. Power Sources* **2001**, *97-98*, 621−623.
(14) Aissou, K.; Mumtaz, M.; Usluer, O.; Pecastaings, G.; Portale, G.; Fleury, G.; Cloutet, E.; Hadziioannou, G. Anisotropic Lithium Ion Conductivity in Signle-Ion Diblock Copolymer Electrolyte Thin Films. *Macromol. Rapid Commun.* **2016**, *37*, 221−226.
(15) Van Humbeck, J. F.; Aubrey, M. L.; Alsbaiee, A.; Ameloot, R.; Coates, G. W.; Dichtel, W. R.; Long, J. R. Tetraarylborate Polymer Networks as Single-Ion Conducting Solid Electrolytes. *Chem. Sci.* **2015**, *6*, 5499−5505.
(16) Rojas, A. A. R.; Inceoglu, S.; Mackay, N. G.; Thelen, J. L.; Devaux, D.; Stone, G. M.; Balsara, N. P. Effect of Lithium-Ion Concentration on Morphology and Ion Transport in Single-Ion-Conducting Block Copolymer Electrolytes. *Macromolecules* **2015**, *48*, 6589−6595.
(17) Inceoglu, S.; Rojas, A. A.; Devaux, D.; Chen, X.; Stone, G. M.; Balsara, N. P. Morphology-Conductivity Relationship of Single-Ion-Conducting Block Copolymer Electrolytes for Lithium Batteries. *ACS Macro Lett.* **2014**, *3*, 510−514.
(18) Thelen, J. L.; Inceoglu, S.; Venkatesan, N. R.; Mackay, N. G.; Balsara, N. P. Relationship between Ion Dissociation, Melt Morphology, and Electrochemical Performance of Lithium and Magnesium Single-Ion Conducting Block Copolymers. *Macromolecules* **2016**, *49*, 9139−9147.
(19) Yin, D.; Horkay, F.; Douglas, J. F.; de Pablo, J. J. Molecular Simulation of the Swelling of Polyelectrolyte Gels by Monovalent and Divalent Counterions. *J. Chem. Phys.* **2008**, *129*, 154902.
(20) Kwon, H.; Zwanikken, J. W.; Shull, K. R.; Olvera de la Cruz, M. Theoretical Analysis of Multiple Phase Coexistence in Polyelectrolyte Blends. *Macromolecules* **2015**, *48*, 6008.
(21) Pryamitsyn, V. A.; Kwon, H. K.; Zwanikken, J. W.; Olvera de la Cruz, J. W. Anomalous Phase Behavior of Ionic Polymer Blends and Ionic Copolymers. *Macromolecules* **2017**, *50*, 5194.
(22) Shen, K.; Wang, Z. G. Electrostatic Correlations and the Polyelectrolyte Self Energy. *J. Chem. Phys.* **2017**, *146*, 084901.
(23) Hall, L. M.; Stevens, M. J.; Frischknecht, A. L. Dynamics of Model Ionomer Melts of Various Architectures. *Macromolecules* **2012**, *45*, 8097−8108.
(24) Hall, L. M.; Stevens, M. J.; Frischknecht, A. L. Effect of Polymer Architecture and Ionic Aggregation on the Scattering Peak in Model Ionomer. *Phys. Rev. Lett.* **2011**, *106*, 127801.
(25) Hexemer, A.; Bras, W.; Glossinger, J.; Schaible, E.; Gann, E.; Kirian, R.; MacDowell, A.; Church, M.; Rude, B.; Padmore, H. A SAXS/WAXS/GISAXS Beamline with Multilayer Monochromator. *J. Phys.: Conf. Ser.* **2010**, *247*, 012007.
(26) Zhang, F.; Ilavsky, J.; Long, G. G.; Quintana, J. P. G.; Allen, A. J.; Jemian, P. R. Glassy Carbon as an Absolute Intensity Calibration Standard for Small-Angle Scattering. *Metall. Mater. Trans. A* **2010**, *41*, 1151.
(27) Ilavsky, J. Nika: Software for Two-Dimensional Data Reduction. *J. Appl. Crystallogr.* **2012**, *45*, 324−328.
(28) Ilavsky, J.; Jemian, P. R. Irena: Tool Suite for Modeling and Analysis of Small-Angle Scattering. *J. Appl. Crystallogr.* **2009**, *42*, 347−353.
(29) Eisenberg, A. M. K. *Ion-Containing Polymers: Physical Properties and Structure*; Academic Press: New York, 1977.
(30) Eisenberg, A. Clustering of Ions in Organic Polymers. A Theoretical Approach. *Macromolecules* **1970**, *3*, 147−154.
(31) Hsu, W. Y.; Gierke, T. D. Ion Transport and Clustering in Nafion Perfluorinated Membranes. *J. Membr. Sci.* **1983**, *13*, 307−326.
(32) Fredrickson, G. H.; Bates, F. S. Dynamics of Block Copolymers: Theory and Experiment. *Annu. Rev. Mater. Sci.* **1996**, *26*, 501−550.
(33) Ferry, J. D. *Viscoelastic Properties of Polymers*, 3rd ed.; John Wiley & Sons: New York, 1980.
(34) Eitouni, H. B.; Balsara, N. P. Effect of Chemical Oxidation on the Self-Assembly of Organometallic Copolymers. *J. Am. Chem. Soc.* **2004**, *126*, 7446−7447.
(35) Teubner, M.; Strey, R. Origin of the Scattering Peak in Microemulsions. *J. Chem. Phys.* **1987**, *87*, 3195−3200.
(36) Schubert, K. V.; Strey, R. Small-angle Neutron Scattering from Microemulsions Near the Disorder Line in Water/Formamide-Octane C_iE_j Systems. *J. Chem. Phys.* **1991**, *95*, 8532−8545.
(37) Martino, A.; Kaler, E. W. Phase Behavior and Microstructure of Nonaqueous Microemulsions. 2. *Langmuir* **1995**, *11*, 779−84.
(38) Ruegg, M. L.; Reynolds, B. J.; Lin, M. Y.; Lohse, D. J.; Balsara, N. P. Minimizing the Concentration of Diblock Copolymer Needed To Organize Blends of Weakly Segregated Polymers by Tuning Attractive and Repulsive Interactions. *Macromolecules* **2007**, *40*, 1207−1217.
(39) Hillmyer, M. A.; Maurer, W. W.; Lodge, T. P.; Bates, F. S.; Almdal, K. Model Bicontinuous Microemulsions in Ternary Homopolymer-Block Copolymer Blends. *J. Phys. Chem. B* **1999**, *103*, 4814−24.
(40) Washburn, N. R.; Lodge, T. P.; Bates, F. S. Ternary Polymer Blends as Model Surfactant Systems. *J. Phys. Chem. B* **2000**, *104*, 6987−97.
(41) Hay, J. N.; Sabir, M.; Steven, R. L. T. Crystallization Kinetics of High Polymers. Polyethylene oxide—Part I. *Polymer* **1969**, *10*, 187−202.
(42) Strobl, G. Crystallization and Melting of Bulk Polymers: New Observations, Conclusions and a Thermodynamic Scheme. *Prog. Polym. Sci.* **2006**, *31*, 398−442.
(43) Hamley, I. W. Crystallization in Block Copolymers, in Interfaces Crystallization Viscoelasticity. *Advances in Polymer Science*; Springer: 1999.
(44) Beaumont, R. H.; Clegg, B.; Gee, G.; Herbert, J. B. M.; Marks, D. J.; Roberts, R. C.; Sims, J. Heat Capacities of Propylene Oxide and of Some Polymers of Ethylene and Propylene Oxides. *Polymer* **1966**, *7*, 401−17.

DOI: 10.1021/acs.macromol.7b01686
Macromolecules 2017, 50, 8765−8776